

# Rotational Doppler effect in left-handed materials

Hailu Luo, Shuangchun Wen,\* Weixing Shu, Zhixiang Tang, Yanhong Zou, and Danyuan Fan  
*Key Laboratory for Micro/Nano Opto-Electronic Devices of Ministry of Education,  
 School of Computer and Communication, Hunan University, Changsha 410082, China*  
 (Dated: October 28, 2018)

We explain the rotational Doppler effect associated with light beams carrying with orbital angular momentum in left-handed materials (LHMs). We demonstrate that the rotational Doppler effect in LHMs is unreversed, which is significantly different from the linear Doppler effect. The physics underlying this intriguing effect is the combined contributions of negative phase velocity and inverse screw of wave-front. In the normal dispersion region, the rotational Doppler effect induces an upstream energy flow but a downstream momentum flow. In the anomalous dispersion region, however, the rotational Doppler effect produces a downstream energy flow but an upstream momentum flow. We theoretically predict that the rotational Doppler effect can induce a transfer of angular momentum of the LHM to orbital angular momentum of the beam.

PACS numbers: 42.25.-p; 42.79.-e; 41.20.Jb; 78.20.Ci

## I. INTRODUCTION

After the first experimental observation of negative refraction [1, 2], some intriguing or even counter-intuitive phenomena in left-handed materials (LHMs), such as amplification of evanescent waves [3, 4], unusual photon tunneling [5, 6], negative Goos-Hänchen shift [7, 8], and reversed linear Doppler effect [9, 10] have attracted much attention. Linear Doppler effect is a well-known phenomenon by which the frequency of a wave is shifted according to the relative velocity of the source and the observer [11]. The conventional understanding of linear Doppler effect is that increased frequencies are measured when a source and an observer approach each other. Applications of the effect are widely established and include radar, laser cooling, flow measurement, and the search for astronomical objects. The inverse linear Doppler effect refers to frequency shifts that are in the opposite sense to those described above. For example, increased frequencies would be measured on reflection of waves from a receding boundary [9, 10].

The interaction of a moving medium with a Laguerre-Gaussian (LG) field raises the fundamental question of the Doppler effect. As a medium moves across the helical wave fronts of the LG field, it experiences, in addition to the usual linear Doppler shift related to the velocity in the light propagation direction, a most intriguing frequency shift, the so-called rotational Doppler effect associated with the azimuthal velocity. The rotational Doppler effect results in frequency shift when the light beam is rotated around its propagation axis. The rotational Doppler effect has been extensively studied in regular right-handed materials (RHMs) [12, 13, 14, 15, 16]. Veselago has suggested that LHMs would reverse nearly all known optical phenomena [17]. Now an interesting question arises: what happens to the rotational Doppler effect in LHMs? When the LG beams incident into

LHMs, the helical wave fronts should reverse their screwing fashion [18]. Thus we can predict that the rotational Doppler effect will result in many intriguing phenomena. The investigation of the rotational Doppler effect will provide insights into the fundamental properties of LHMs and will allow us to better understand the interaction of light with LHMs.

In this work, we try to reveal the rotational Doppler effect associated with light beams carrying orbital angular momentum in LHMs. First, starting from the Maxwell's equations in moving frame, we obtain the analytical description for LG beams propagating in rotating LHMs. Our formalism permits us to introduce the effective index to describe the wave propagation. Next, we attempt to recover how the wave-front evolves, and how the screwing wave-fronts result in upshifted and downshifted frequencies. In order to explore the rotational Doppler effect, we examine a simplest intensity pattern formed by LG beams with equal magnitudes and waist parameters. Then, we want to investigate how the rotational Doppler effect gives rise to the anomalous upstream transverse Poynting vector and angular momentum flow. Finally, we attempt to explore how the rotational Doppler effect influences the rotation of intensity pattern inside the LHM.

## II. EFFECTIVE REFRACTIVE INDEX

To investigate the effective index of rotating LHM, we firstly use the Maxwell's equations to determine the field distribution inside the LHM. We consider a monochromatic electromagnetic field,  $\mathbf{E}(\mathbf{r}, t) = \text{Re}[\mathbf{E}(\mathbf{r}) \exp(-i\omega t)]$  and  $\mathbf{B}(\mathbf{r}, t) = \text{Re}[\mathbf{B}(\mathbf{r}) \exp(-i\omega t)]$ , of angular frequency  $\omega$  propagating from a conventional RHM to the LHM. The field can be described by Maxwell's equations

$$\begin{aligned} \nabla \times \mathbf{E} &= -\frac{\partial \mathbf{B}}{\partial t}, & \nabla \cdot \mathbf{B} &= 0, \\ \nabla \times \mathbf{H} &= \frac{\partial \mathbf{D}}{\partial t}, & \nabla \cdot \mathbf{D} &= 0. \end{aligned} \quad (1)$$

\*Electronic address: scwen@hnu.cn

From the Maxwell's equations, we can easily find that the wave propagation is permitted in materials with  $\varepsilon < 0$  and  $\mu < 0$ . Veselago termed these LHMs, because the vectors  $\mathbf{E}$ ,  $\mathbf{H}$  and  $\mathbf{k}$  form a left-handed triplet instead of a right-handed triplet, as is the case in regular RHMs [17].

In order to investigate the effective index, we introduce a rest frame and a moving frame [19]. In the rest frame the LHM rotates with an angular velocity  $\mathbf{v}_\varphi = \boldsymbol{\Omega} \times \mathbf{r}$  and in the moving frame the LHM is at rest. We restrict our analysis to a small velocity with  $v \ll c$ . For the LHM at rest, we have the following constitutive relations:

$$\mathbf{D}' = \varepsilon_0 \varepsilon(\omega') \mathbf{E}' \quad \mathbf{B}' = \mu_0 \mu(\omega') \mathbf{H}' \quad (2)$$

where we have used primes to denote the fields and their frequencies in the moving frame. The fields in the moving frame can be expressed in the rest frame by a Lorentz transformation, which gives to first order in  $v/c$ :

$$\mathbf{D} + \frac{\mathbf{v} \times \mathbf{H}}{c^2} = \varepsilon_0 \varepsilon(\omega) (\mathbf{E} + \mathbf{v} \times \mathbf{B}), \quad (3)$$

$$\mathbf{B} - \frac{\mathbf{v} \times \mathbf{E}}{c^2} = \mu_0 \mu(\omega) (\mathbf{H} - \mathbf{v} \times \mathbf{D}). \quad (4)$$

Here electric permittivity  $\varepsilon$  and magnetic permeability  $\mu$  are given as a function of the frequency in the moving frame. We also assume that  $\varepsilon$  and  $\mu$  depend only on the frequency and is independent of the state of motion of the LHM. On combining these two equations, we can obtain the following wave equation:

$$\nabla^2 D = -n(\omega'_\pm)^2 \omega^2 D + 2[n(\omega'_\pm)^2 - 1]\Omega \omega (\sigma \pm \partial_\varphi) D, \quad (5)$$

where we have introduced the relation  $n(\omega') = -\sqrt{\varepsilon(\omega')\mu(\omega')}$ , and  $\sigma = \pm 1$  corresponds to left- and right-handed circularly polarized light, respectively. To determine the effective indices, we solve the wave equation for helical wave-front LG beams.

We introduce the Lorentz-gauge vector potential to describe the propagation characteristics of LG filed. The vector potential of the beam propagating in the  $+z$  direction can be written in the form

$$\mathbf{A} = A_0(\alpha \mathbf{e}_x + \beta \mathbf{e}_y) u_{p,l}(\mathbf{r}) \exp(ink_0 z - i\omega t). \quad (6)$$

Here  $A_0$  is a complex amplitude,  $n$  is the effective index,  $k_0 = \omega/c$ ,  $c$  is the speed of light in vacuum,  $\mathbf{e}_x$  and  $\mathbf{e}_y$  are unit vectors, respectively. The coefficients  $\alpha$  and  $\beta$  satisfy the relation  $\sigma = i(\alpha\beta^* - \alpha^*\beta)$ . It is well known that each photon in a light beam carries a spin angular momentum.

To be uniform throughout the following analysis, we introduce different coordinate transformations  $z_i^*(i = 1, 2)$  in the RHM and the LHM, respectively. The field can be written as

$$\begin{aligned} u_{pl} = & \frac{C_{pl}}{w(z_i^*)} \left[ \frac{\sqrt{2}r}{w^2(z_i^*)} \right]^l L_p^l \left[ \frac{\sqrt{2}r}{w^2(z_i^*)} \right] \exp \left[ \frac{-r^2}{w^2(z_i^*)} \right] \\ & \times \exp \left[ \frac{-ink_0 r^2 z_i^*}{R(z_i^*)} \right] \exp[\pm il\varphi] \\ & \times \exp[-i(2p + l + 1) \arctan(z_i^*/z_R)], \end{aligned} \quad (7)$$

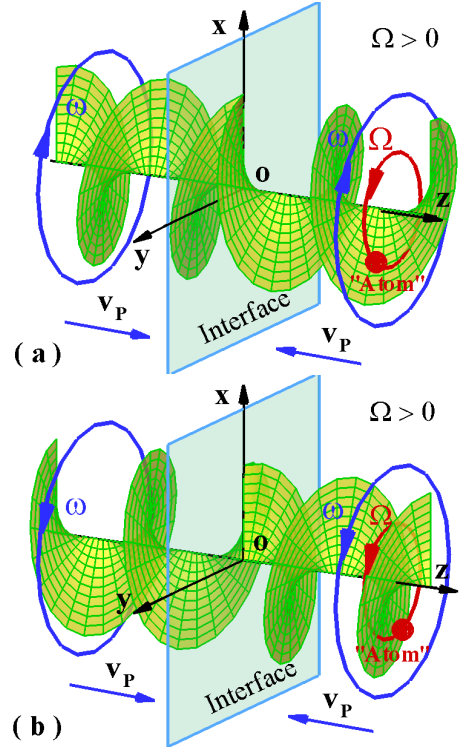


FIG. 1: (Color online) The helical wave front for Laguerre-Gaussian beam result from an azimuthal phase structure of  $\exp[\pm il\varphi]$ . The LHM is rotating with angular velocity  $\Omega$ . The phase velocity  $\mathbf{v}_P$  reverses its direction and the wave-fronts reverse their screwing rotation in the LHM. When a metamaterial “atom” moves across the helical wave fronts, it experiences the so-called rotational Doppler effect. (a) The helical wave front with  $\exp[+i\varphi]$  and the effective frequency  $\omega' = \omega + \Omega$ . (b) The helical wave front with  $\exp[-i\varphi]$  and the effective frequency  $\omega' = \omega - \Omega$ .

$$w(z_1^*) = w_0 \sqrt{1 + (z_i^*/z_R)^2}, \quad R(z_i^*) = z_i^* + \frac{z_R^2}{z_i^*}. \quad (8)$$

Here  $C_{pl}$  is the normalization constant,  $L_p^l[2r^2/w^2(z_1^*)]$  is a generalized Laguerre polynomial,  $z_R = nk_0 w_0^2/2$  is the Rayleigh length, and  $w(z_i^*)$  is the beam size and  $R(z_i^*)$  the radius of curvature of the wave front. The last term in Eq. (7) denotes the Gouy phase which is given by  $\Phi = -(2p + l + 1) \arctan(z_i^*/z_R)$ .

Now let us study the screw of the wave front. Here the sense of the positive angles is chosen as anticlockwise, while negative angles are considered in the clockwise direction. In the rotating LHM, the constant wavefront satisfies

$$n_+ k_0 z_i^* + \frac{-in_+ k_0 r^2}{R_+(z_i^*)} + l\varphi + \Phi_+(z_i^*) = \text{const}, \quad (9)$$

$$n_- k_0 z_i^* + \frac{-in_- k_0 r^2}{R_-(z_i^*)} - l\varphi + \Phi_-(z_i^*) = \text{const}. \quad (10)$$

The schematic view of the wave front is a three-dimensional screw surface of  $(r \cos \varphi, r \sin \varphi, z)$ . The plotting range of  $r$  is from 0 to  $5w_0$  with the interval of

$\Delta r = 0.5w_0$  and that of  $|n_{\pm}|k_0z$  is from 0 to  $4\pi$  with the interval of  $|n_{\pm}|k_0\Delta z = 0.1\pi$ . The wavefront structure reverse their screw types with a pitch of  $\lambda_0/|n_{+}|$  and  $\lambda_0/|n_{-}|$ , respectively (see Fig. 1).

The helical wave fronts with clockwise or anticlockwise screwing fashion will result in different effective indices. Substituting the LG beam in the wave equation, we have

$$k_{\pm}^2(\omega) = n^2(\omega'_{\pm})\frac{\omega^2}{c^2} - 2[n^2(\omega'_{\pm}) - 1]\frac{\Omega\omega}{c^2}(\sigma \pm l). \quad (11)$$

Thus from Eq. (11), and using the relation  $k(\omega) = n(\omega')\omega/c$ , we can obtain an equation of the refractive indices associated with the waves of each screwing fashion:

$$n_{\pm}(\omega) = n(\omega'_{\pm}) - \left[ n(\omega'_{\pm}) - \frac{1}{n(\omega'_{\pm})} \right] \frac{\Omega}{\omega}(\sigma \pm l). \quad (12)$$

Here we have approximated the refractive indices to the first order in  $\Omega/\omega$ . To obtain the indices, we need to know the effective frequency. Strictly speaking, we cannot obtain it from the wave equation in the moving frame. Now a question arises: how to determine the value of effective frequency in the LHM?

### III. ROTATIONAL DOPPLER EFFECT

In the case of electromagnetic radiation this usually means that the subunits must be much smaller than the wavelength of radiation. Then the unit cells of metamaterials can be modeled as the atoms (or molecules) in ordinary materials. In particular, electric atoms with an electric-dipole moment leading to a negative electric permittivity, and magnetic atoms with a magnetic-dipole moment leading to a negative magnetic permeability. Hence the rotational Doppler effect in LHMs is the result of the optical properties of the individual metamaterial “atoms” (see Fig. 1).

To quantify the changes that occur in the Doppler effect for metamaterial “atoms” interacting with light beams with orbital angular momentum, the quantum mechanical derivation [13] is developed for describing the rotational Doppler effect in LHMs. The Doppler shift experienced by a LG field in a moving frame is given by

$$\delta_{LG} = \left[ -nk_0 + \frac{nk_0r^2}{2(z_i^2 + z_R^2)} \left( \frac{2z_i^2}{z_i^2 + z_R^2} - 1 \right) - \frac{(2p+l+1)z_R}{z_i^2 + z_R^2} \right] v_z - \frac{nk_0r}{R} v_r - \frac{\sigma \pm l}{r} v_{\varphi} \quad (13)$$

where  $v_z$ ,  $v_r$ , and  $v_{\varphi}$  are the axial, radial, and azimuthal velocity components of the metamaterial “atom”, respectively. The axial Doppler shift is obtained from  $nk_0v_z$ . There are two additional terms which account for the radial phase and the Gouy-phase. Note that the two additional terms should be reversed, since the negative index and the inverse Gouy-phase shift [20]. Thus we can conclude that the linear Doppler effect associated with

light beams is slightly different from the counterpart of plane wave [9, 10]. Further investigation shows that the radial Doppler shift, given by the term proportional to  $v_r$ , should also be reversed in LHMs.

A most intriguing frequency shift, the so-called rotational Doppler effect arises from the azimuthal velocity  $v_{\varphi} = \Omega r$ . The rotational Doppler effect results in frequency shift when the light beam is rotated around its propagation axis. The corresponding rotational Doppler shift in LHMs is given by  $\delta_{LG}^{\varphi} = (\sigma \pm l)\Omega$ , which is proportional to the total angular momentum. It can be seen that beams propagate differently in a rotating LHM, depending on whether the wave fronts turn in the same rotation sense as the LHM or in the opposite sense. The frequency of an incident LG beam whose wave-front is screwing as the LHM is downshifted to  $\omega' = \omega - (\sigma + l)\Omega$ , whereas a LG beam of the opposite sense is upshifted to  $\omega' = \omega - (\sigma - l)\Omega$ . Unexpectedly, the rotational frequency shift in LHMs is unreversed.

When a LG beam incident into a LHM, the helical wave fronts reverse their screwing fashion [18]. Why is the rotational frequency shift unreversed? By closely examining the evolution of wave-front, we find the phase velocity also inverses its direction (see Fig. 1). Hence the dynamic evolution between the metamaterial “atom” and wave-front remains unchanged. We conclude that the physics underlying the unreversed effect is collective contributions of negative phase velocity and inverse screw of wave-front.

Though the rotational Doppler effect is unreversed, much more counter-intuitive phenomena will be caused in the LHMs. In order to explore the rotational Doppler effect, we will examine a simplest intensity pattern which is formed by  $LG_{0,+1}$  and  $LG_{0,-1}$  beams with equal magnitudes and waist parameters. In principle, any arbitrary light beam can be described by a superposition of LG modes [21]. In the case of equal frequencies, such a combination is well known to be equivalent to an ordinary Hermite-Gaussian (HG) beam with a double-spot intensity distribution. We will explore the energy flow and angular momentum flow caused by rotational Doppler effect.

First let us examine the propagation characteristics of energy flow, which is usually discussed by use of the Poynting vector. There has been considerable interest in orbital angular momentum of LG beams relating to azimuthal component of Poynting vector [22, 23, 24]. The time average Poynting vector,  $\mathbf{S}$ , can be written as

$$\mathbf{S} = \frac{1}{2} \text{Re}[(\mathbf{E}_{+} + \mathbf{E}_{-}) \times (\mathbf{H}_{+} + \mathbf{H}_{-})^*]. \quad (14)$$

We denote the radial, azimuthal, and axial components of the vector  $\mathbf{S}$  in the cylindrical coordinates by the notation  $S_r$ ,  $S_{\varphi}$ , and  $S_z$ , respectively. The component  $S_r$ , relates to the spread of the beam as it propagates. The azimuthal component  $S_{\varphi}$  describes the energy flow that circulates around the propagating axis. The axial component  $S_z$  describes the energy flow that propagates along the  $+z$  axis.

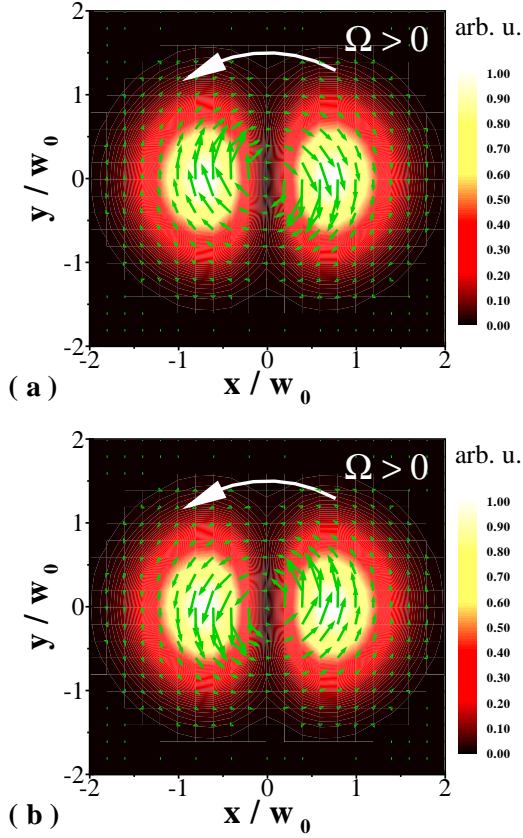


FIG. 2: (Color online) In the normal dispersion region, the rotational Doppler effect induces (a) the downstream energy flow and (b) the anomalous upstream transverse momentum flow. The parameters are  $\omega = 1.366\omega_0$  and  $z_2^* = 0$ . The green arrows denote the transfers Poynting vector and momentum flow. Please note that the beam divergence is not shown due to normalization of transverse dimension.

Next we attempt to describe the evolution of momentum flow. The momentum flow for the electromagnetic wave can be written in the form [11]

$$\mathbf{T} = \frac{1}{2} \text{Re}[(\mathbf{D} \cdot \mathbf{E}^* + \mathbf{B} \cdot \mathbf{H}^*)\mathbf{I} - (\mathbf{D}\mathbf{E}^* + \mathbf{B}\mathbf{H}^*)]. \quad (15)$$

Here  $\mathbf{T}$  is the momentum flow also referred as the Maxwell stress tensor, and  $\mathbf{I}$  is  $3 \times 3$  identity matrix. For a HG beam,  $\mathbf{E} = \mathbf{E}_+ + \mathbf{E}_-$  and  $\mathbf{H} = \mathbf{H}_+ + \mathbf{H}_-$ . Note that the momentum flow is significantly different from that obtained by Minkowski or Abraham momentum [11]. The cross product of this momentum density with the radius vector yields an orbital angular momentum flow. The orbital angular momentum flow in the  $z$  direction depends upon the component of  $\mathbf{T}_\varphi$ , such that  $\mathbf{J}_z = \mathbf{r} \times \mathbf{T}_\varphi$ .

In order to accurately describe the Poynting vector and momentum flow, it is necessary to include material dispersion and losses [25]. Thus, a certain dispersion relation, such as the Lorentz medium model, should be

introduced. The constitutive parameters are

$$\varepsilon(\omega) = \varepsilon_0 \left( 1 - \frac{\omega_{ep}^2}{\omega^2 - \omega_{eo}^2 + i\omega\gamma_e} \right), \quad (16)$$

$$\mu(\omega) = \mu_0 \left( 1 - \frac{F\omega_{mp}^2}{\omega^2 - \omega_{mo}^2 + i\omega\gamma_m} \right). \quad (17)$$

To avoid the trouble involving in a certain value of frequency, we assume the material parameters are  $\omega_{eo} = \omega_{mo} = \omega_o$ ,  $\omega_{ep}^2 = F\omega_{mp}^2 = 2\omega_o^2$  and  $\gamma_e = \gamma_m = 0.25\omega_0$ . It should be noted that, as we will see in the following, the dispersion and negative indices will play a very important role in the rotation of Poynting vector and momentum flow.

Figure 2 shows the characteristics of Poynting vector and momentum flow. The circumstance is really intriguing: the novel azimuthal energy flow and momentum flow present in the HG field. Counter-intuitively, the angular velocity  $\Omega$  of the rotating LHM and the circulation of Poynting vector are opposite, as shown in Fig. 2(a). The presence of the azimuthal momentum flow  $\mathbf{T}_\varphi$  has been identified as the orbital angular momentum. We thus predict that the rotational Doppler effect can induce a transfer of angular momentum of the LHM to obitual angular momentum of the beam. The sign of the orbital angular momentum coincides with handedness of rotation of the LHM. Positive orbital angular momentum is associated with the counter-clockwise rotation  $\Omega > 0$ , as plotted in Fig. 2(b). On the contrary, the sign of the orbital angular momentum in the HG field is negative: when the LHM rotates clockwise  $\Omega < 0$ , the angular momentum flow seemingly corresponds to the clockwise circulation. The physical origin of transfer of angular momentum is rooted in the geometric phase difference between  $\text{LG}_{0,+1}$  and  $\text{LG}_{0,-1}$  beams.

Whether the rotational Doppler effect induce the downstream or upstream angular momentum depends on the normal or anomalous dispersion. In the normal dispersion region,  $\partial \text{Re}[n(\omega)]/\partial \omega > 0$ , the rotational Doppler effect induces a upstream energy flow [see Fig. 2(a)] but a downstream momentum flow [see Fig. 2(b)]. In the anomalous dispersion region,  $\partial \text{Re}[n(\omega)]/\partial \omega < 0$ , however, the rotational Doppler effect induces a downstream energy flow and a upstream momentum flow. Interestingly, we find that the transverse energy flow in the LHM is antiparallel to the transverse momentum flow. In our opinion, the main reason for such an inconsistency is the negative refractive index. Note that the novel phenomenon is significantly different from the counterpart in regular RHM [26].

To understand a better physical picture, let us reveal the instant field distribution in the LHM. The rotation of the intensity pattern in LHM arises from the difference in the refractive indices for constituent LG beams. The transverse beam pattern is determined by the geometric phase difference:

$$\Delta k z_i^* + \frac{k_+ r^2}{R_+(z_i^*)} - \frac{k_- r^2}{R_-(z_i^*)} + 2l\varphi - \Delta\Phi = \text{const}, \quad (18)$$

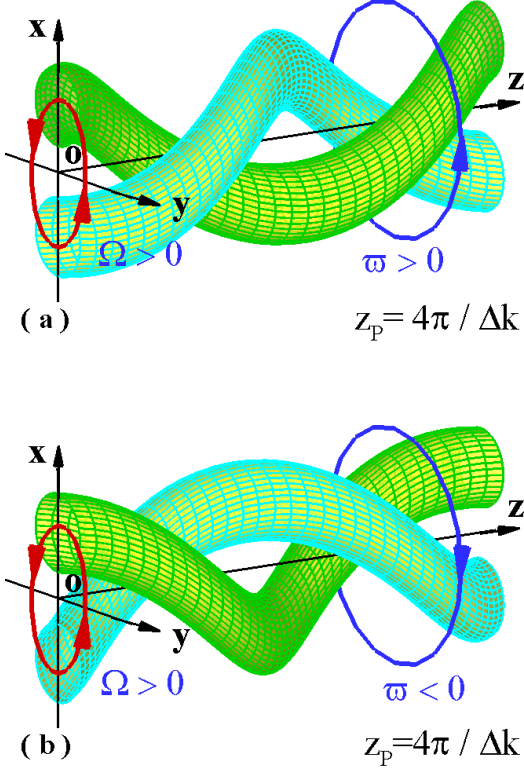


FIG. 3: (Color online) Instant spatial structure of HG beam screws with pitch  $z_p = 4\pi/(k_+ - k_-)$  in the LHM. The rotational Doppler effect induces rotation of intensity pattern: (a) the downstream rotation ( $\Omega > 0$ ,  $\varpi > 0$ ) in normal dispersion region, (b) the upstream rotation ( $\Omega > 0$ ,  $\varpi < 0$ ) in anomalous dispersion region. Please note that the beam divergence is not shown due to normalization of transverse dimension.

where  $\Delta k = k_+ - k_-$ ,  $k_{\pm} = n_{\pm}(\omega')\omega/c$ , and  $\Delta\Phi = \Phi_+ - \Phi_-$ . The schematic view of the spatial structure of instant field is plotted in Fig. 3. Here we have neglected the phase difference caused by radial and Gouy phases. The spatial structure exhibits a screwing type with a pitch of  $z_p = 4\pi/(k_+ - k_-)$  along the  $+z$  axis.

In this case, the constituent LG beams propagate differently in the LHM which leads to a change in their relative phase. The pattern rotates with an angular velocity  $\varpi = c(k_+ - k_-)/2$ . The angle per unit length by which the intensity pattern is rotated is called the specific rotary power  $\Delta\theta_l = 2\pi(n_+ - n_-)/\lambda$ . Hence the rotational Doppler effect induces a downstream or a upstream rotation of the intensity pattern, depending on whether the frequency locates in the region of normal or anomalous dispersion. In the normal dispersion region,  $k_+ > k_-$ , the angular velocity  $\varpi > 0$ , and the rotational Doppler effect induces a downstream rotation of intensity pattern [see Fig. 3(a)]. In the anomalous dispersion region,  $k_+ < k_-$ , the angular velocity  $\varpi < 0$ , and the rotational Doppler effect induces a downstream rotation of intensity pattern [see Fig. 3(b)]. A further point should

be mentioned that the large rotation can be obtained if  $k_+$  and  $k_-$  have opposite signs (i.e.,  $k_+ > 0$ ,  $k_- < 0$  or  $k_+ < 0$ ,  $k_- > 0$ ). Our result suggests that the interesting images rotation [27, 28, 29] might more readily be accessed in LHMs.

The possibility of having an upstream rotation of intensity pattern in the presence of anomalous dispersion, i.e., in the presence of negative group velocity. As negative group velocities in dispersive media are forbidden by Kramers-Kronig relations in all frequency regions [11]. Thus negative group velocities are possible only in the presence of absorption. In a recent experiment [30], the negative group velocity have been demonstrated by observing that the pulse advances in time with respect to the same wave packet propagating in vacuum. The low-loss LHMs are therefore good candidates for the experimental observation of significant upstream rotation of intensity pattern. Conversely, the anomalous upstream rotation of intensity pattern could provide an interesting way to reveal the nature of LHMs.

#### IV. CONCLUSIONS

In conclusion, we have investigated the rotational Doppler effect associated with light beams carrying orbital angular momentum in LHMs. Unlike the reversed linear Doppler effect, the rotational Doppler effect in LHMs is unreversed. We have revealed that the physics underlying this intriguing effect is combined contributions of negative phase velocity and inverse screw of wavefront. Though the rotational Doppler effect is independent of the refractive index, much more counter-intuitive phenomena will be caused in the LHMs. In the normal dispersion region, the rotational Doppler effect induces a downstream energy flow but a upstream momentum flow. In the anomalous dispersion region, however, the rotational Doppler effect induces a upstream energy flow but a downstream momentum flow. We theoretically predict that the rotational Doppler effect can induce a transfer of angular momentum of the LHM to orbital angular momentum of the beam. It is possible that the study of Poynting vector and momentum flow in LHMs may make a useful contribution to long established Abraham-Minkowski dilemma. We have shown that the momentum flow in LHMs should be antiparallel to the Poynting vector. Thus the direction of momentum flow is significantly different from that obtained by Minkowski or Abraham momentum. We consider that this difference might help us to illustrate this long established problem.

#### Acknowledgments

This work was supported by projects of the National Natural Science Foundation of China (Grants Nos. 10576012, 10674045, and 60538010).

- 
- [1] D. R. Smith, W. J. Padilla, D. C. Vier, S. C. Nemat-Nasser, S. Schultz, Phys. Rev. Lett. **84**, 4184 (2000).
  - [2] R. A. Shelby, D. R. Smith, S. Schultz, Science **292**, 77 (2001).
  - [3] J. B. Pendry, Phys. Rev. Lett. **85**, 3966 (2000).
  - [4] N. Fang, H. Lee, C. Sun, and X. Zhang, Science **308**, 534 (2005).
  - [5] Z. M. Zhang and C. J. Fu, Appl. Phys. Lett. **80**, 1097 (2002).
  - [6] K. Y. Kim, Phys. Rev. E **70**, 047603 (2004).
  - [7] J. A. Kong, B. Wu, and Y. Zhang, Appl. Phys. Lett. **80**, 2084 (2002).
  - [8] P. R. Berman, Phys. Rev. E **66**, 067603 (2002).
  - [9] N. Seddon and T. Bearpark, Science **302**, 1537 (2003).
  - [10] Daniel D. Stancil, Benjamin E. Henty, Ahmet G. Cepni, and J. P. Van't Hof, Phys. Rev. E **74**, 060404(R)(2006).
  - [11] J. D. Jackson, *Classical Electrodynamics* (Wiley, New York, 1999).
  - [12] B. A. Garetz and S. Arnold, Opt. Commun. **31**, 1 (1979).
  - [13] L. Allen, M. Babiker, and W. L. Power, Opt. Commun. **112**, 141 (1994).
  - [14] G. Nienhuis, Opt. Commun. **132**, 8 (1996).
  - [15] J. Courtial, K. Dholakia, D. A. Robertson, L. Allen, and M. J. Padgett, Phys. Rev. Lett. **80**, 3217 (1998).
  - [16] J. Courtial, D. A. Robertson, K. Dholakia, L. Allen, and M. J. Padgett, Phys. Rev. Lett. **81**, 4828 (1998).
  - [17] V. G. Veselago, Sov. Phys. Usp. **10**, 509 (1968).
  - [18] H. Luo, Z. Ren, W. Shu, and S. Wen, Phys. Rev. A **77**, 023812 (2008).
  - [19] M. A. Player, Proc. R. Soc. London Ser. A **349**, 441 (1976).
  - [20] H. Luo, Z. Ren, W. Shu, and F. Li, Phys. Rev. E **75**, 026601 (2007).
  - [21] L. Allen, S. M. Barnett, and M. J. Padgett, *Optical Angular Momentum* (IOP Publishing Ltd., London, Cambridge, 2003) and references therein.
  - [22] L. Allen, M. W. Beijersbergen, R. J. C. Spreeuw, and J. P. Woerdman, Phys. Rev. A **45**, 8185 (1992).
  - [23] M. J. Padgett and L. Allen, Opt. Commun. **121**, 36 (1995).
  - [24] L. Allen and M. J. Padgett, Opt. Commun. **184**, 67 (2000).
  - [25] B. A. Kemp, J. A. Kong and T. M. Grzegorzczak, Phys. Rev. A **75**, 053810 (2007).
  - [26] A. Yu. Bekshaev, M. S. Soskin, and M. V. Vasnetsov, Opt. Commun. **249**, 367 (2005).
  - [27] M. J. Padgett, G. Whyte, J. Girkin, A. Wright, L. Allen, P. Ohberg, and S. M. Barnett, Opt. Lett. **31**, 2205 (2006).
  - [28] J. B. Götte, S. M. Barnett, M. Padgett, Proc. R. Soc. London, Ser. A **463**, 2185, (2007).
  - [29] J. Leach, A. J. Wright, J. B. Götte, J. M. Girkin, L. Allen, S. Franke-Arnold, S. M. Barnett, and M. J. Padgett, Phys. Rev. Lett. **100**, 153902 (2008).
  - [30] G. Dolling, D. Enkrich, M. Wegener, C. M. Soukoulis, and S. Linden, Science **312**, 892 (2006).